



Theoretical Study of Cluster Ions Existing in Vapours over Cesium Bromide and Iodide

Stanley F. Mwangi^{1*}, Tatiana P. Pogrebnyaya¹ and Alexander M. Pogrebnoi¹

¹Department of Materials, Energy Science and Engineering, Nelson Mandela African Institution of Science and Technology (NM-AIST), Arusha, Tanzania.

Authors' contributions

This work was carried out in collaboration between all authors. Author SFM performed computations, wrote the first draft of the manuscript and managed literature searches. Author TPP performed corrections and some selected computations regarding the structure and vibrational spectra. Author AMP performed some selected thermodynamic calculations. All authors analyzed and discussed the results and approved the final manuscript.

Article Information

DOI: 10.9734/BJAST/2015/17612

Editor(s):

(1) Shyang Chow Wen, School of Materials and Mineral Resources Engineering, Engineering Campus, Universiti Sains Malaysia, Malaysia.

Reviewers:

(1) Yongchun Zhu, Chemistry Department, Shenyang Normal University, China.

(2) Anonymous, Kastamonu University, Turkey.

Complete Peer review History: <http://www.sciencedomain.org/review-history.php?id=1137&id=5&aid=9221>

Original Research Article

Received 20th March 2015

Accepted 20th April 2015

Published 13th May 2015

ABSTRACT

The properties of ions Cs_2X^+ , Cs_3X_2^+ , CsX_2^- , and Cs_2X_3^- (X = Br or I) have been studied using the density functional theory and Möller–Plesset perturbation theory of the 2nd and 4th order. For all species the equilibrium geometrical configurations and vibration frequencies were determined. Different isomers of pentaatomic ions were found to exist: the linear ($D_{\infty h}$), V-shaped (C_{2v}), kite-shaped (C_{2v}) and bipyramidal (D_{3h}). The relative abundances of isomers were calculated for temperatures between 700 K and 1600 K. It was found that at about 800 K, the amount of different isomers was comparable for Cs_3Br_2^+ , Cs_3I_2^+ and Cs_2I_3^- ions, while for Cs_2Br_3^- the linear isomer was proved to be predominant. The enthalpies of dissociation reactions with elimination of CsX molecules and the enthalpies of formation of ions were determined.

Keywords: Cluster ions; cesium bromide; cesium iodide; isomers; enthalpies of formation of ions; enthalpies of dissociation reactions.

*Corresponding author: E-mail: ferdinands@nm-aist.ac.tz;

1. INTRODUCTION

Alkali halide cluster ions form a potential group for researches due to the possibilities of designing and fabricating new materials. Some of these cluster ions have unique properties such as electronic, optical and magnetic which are function of size and composition [1-3]. These species can serve as fundamental building blocks for a new class of materials with desired properties [3,4].

Different species composed of cesium and iodine are proved to exist among the fission products that can be released in nuclear power plants [5-8]. They have major impact on ground contamination and radiation doses in the environment in case of accidents such as containment building leakages. They are highly radioactive in short term for iodine and in middle term for cesium [5,6,9]. Thus, evaluations of their thermodynamic properties are essential for safety features of the nuclear pressurized water reactor.

Considerable studies of alkali halide cluster ions have been done in the past decades [4,10-15]. Different analytical procedures have been employed for the investigation of ionic clusters [16,17]. Mass spectrometry stands as a major experimental technique which is capable of analyzing a broad characterization of their properties [18]. Various positive and negative ions had been identified in equilibrium vapours using high temperature mass spectrometry [19-25]. For the treatment of experimental data thermodynamic functions of molecules and ions are required and for the calculation of the thermodynamic functions the geometrical parameters and vibrational frequencies are needed. However they are difficult to be measured by available experimental techniques [26].

Quantum chemical methods are proficient to provide accurate information required. Previously the structure and properties of cluster ions existing in saturated vapors over sodium fluoride (NaF), sodium chloride (NaCl), sodium bromide (NaBr) sodium iodide (NaI), potassium chloride (KCl), rubidium chloride (RbCl) and cesium chloride (CsCl) had been studied by Pogrebnaya et al., [27-30] using quantum chemical methods.

The ionic species Cs^+ , Cs_2I^+ , Cs_3I_2^+ , I^- , CsI_2^- , and Cs_2I_3^- have been detected in the saturated

vapour over cesium iodide by high temperature mass spectrometry [24,31]. Photoelectron spectroscopy was applied to CsI_2^- [32]. The ions Cs_2I^+ and CsI_2^- were resulted from collisions of Cs_2I_2 with Xe [33]. In line to this, we expect similar ions to exist in saturated vapour over cesium bromide. Thus the aims of the present work were to determine the characteristics of the cluster ions of cesium bromide and iodide using quantum chemical methods, as well as to calculate the thermodynamic properties of the ions. To verify the reliability of the results obtained, the properties of neutral species CsX and Cs_2X_2 have been calculated and analyzed through a comparison with the available reference data.

2. COMPUTATIONAL DETAILS

The calculations were performed by GAMESS (General Atomic and Molecular Electronic Structure System) program [34], Firefly version 8.0.0 [35], employing electron density functional theory (DFT) with the Becke–Lee–Yang–Parr functional (B3LYP5) [36,37] and Becke-Perdew functional (B3P86) [37-39], as well as the second order and fourth order Möller–Plesset perturbation theory (MP2 and MP4). The effective core potential (Cs ECP GEN 46 3, 9 electrons in the core) with Def2-QZVP basis set (6s5p4d1f) [40] for Cs and the relativistic effective core potentials (Br ECP GEN 28 4, 7 electrons in the core; I ECP GEN 46 4, 7 electrons in the core) with SDB-aug-cc-pVTZ basis set (4s4p3d2f) [41] taken from EMSL (The Environmental Molecular Sciences Laboratory, U.S.) [42-44] were used. The B3LYP5 and MP2 methods were applied to compute the geometrical parameters and vibrational spectra of cluster ions. The geometrical structures determined are confirmed as corresponding to minima energy by the absence of imaginary frequencies.

The dissociation energies $\Delta_r E$ were calculated by B3LYP5, B3P86 and MP2 methods. Also more advanced MP4 level was employed, the equilibrium geometrical structure found by MP2 method was used. Furthermore, the correction for basis set superposition error (BSSE) [45] has been taken into account for MP2 and MP4 methods using the procedure proposed in [46]. The methods of calculations with BSSE corrections are denoted hereafter as MP2C and MP4C.

3. RESULTS AND DISCUSSION

3.1 Molecular Properties of CsX and Cs₂X₂ (X = Br or I)

For the monomer molecules CsBr and CsI, the properties such as geometrical parameters, normal vibrational frequencies, dipole moments and ionization energies have been computed using the B3LYP5 and MP2 methods. The results are compared with available reference data (Table 1) which include the experimental [47,48] and found by a high level quantum chemical calculation [6] as well. For both CsBr and CsI molecules, the internuclear distances $R_e(\text{Cs-X})$ calculated by us are longer than the reference values. The B3P86 method gives better results when comparing with the values obtained from microwave spectrum however overestimating it by 0.02 Å for both CsBr and CsI. While the MP2 method is also close to the experimental value of microwave spectrum since it was longer by 0.03 Å for CsBr and 0.04 Å for CsI. The difference in the reference data themselves are about 0.02 Å for CsBr and 0.01 Å for CsI. The calculated values of the normal vibrational frequencies ω_e are related to the internuclear separations: the bigger is the distance, the smaller the frequency. The values of frequencies computed by all three methods B3LYP5, MP2 and B3P86 are in agreement with the reference values, the MP2 being preferred.

The ionization energies were calculated as energy differences between the parent and ionized species. The results obtained by three theoretical levels are in agreement between each other and with the experimental values [47-50] as well. As for the dipole moment, the theoretical results do not contradict to the experimental

data, the B3LYP5 level being in better agreement.

For the dimer molecules Cs₂Br₂ and Cs₂I₂ the structure was proved to be planar cycle (rhomb) with symmetry D_{2h} (Fig. 1a) that is in accordance with Hargittai [51] and Dickey et al. [52] reported that all dimers geometries of alkali halides have D_{2h} symmetry. The calculated and reference data for Cs₂X₂ molecules are gathered in Table 2: geometrical parameters, vibrational frequencies, IR intensities and enthalpies of dissociation.

The internuclear distances $R_e(\text{Cs-X})$ found by MP2 and both DFT methods are in agreement with the literature values taking into account the scatter of about 0.06 Å of the reference data themselves. It is worth to mention that following the general trend in our data which are usually overrated compared with reference values, the theoretical results by Badawi et al. [6], $R_e(\text{Cs-Br}) = 3.296$ Å and $R_e(\text{Cs-I}) = 3.511$ Å, seem to be more realistic and preferable for both dimers while the experimental values of $R_e(\text{Cs-Br}) = 3.356$ Å found by electron diffraction study [48] and $R_e(\text{Cs-I}) = 3.572$ Å [53] both look overrated.

The experimental vibrational frequencies are confined by two values of ω_1 (A_g) and ω_6 (B_{3u}) for Cs₂Br₂ [50] and four values ω_1 (A_g), ω_4 (B_{1u}), ω_5 (B_{2u}), and ω_6 (B_{3u}) for Cs₂I₂ [50,53,54]. The theoretical values of ω_i [6] are taken into account as well. We can notice that theoretical frequencies computed by us are in a good agreement with the reference values.

Concluding this section about the geometrical parameters and frequencies of the dimer molecules, we can state that all three methods, B3LYP5, B3P86 and MP2, give reasonable results in most cases, nevertheless MP2 method provides less deviation from the reference data.

Table 1. Calculated and literature data of the CsX (X = Br or I) molecules

Property	CsBr				CsI			
	B3LYP5	B3P86	MP2	Reference	B3LYP5	B3P86	MP2	Reference
$R_e(\text{Cs-X}), \text{Å}$	3.124	3.094	3.105	3.072 [48, 49] ^a 3.099 [48] ^b 3.087 [6] ^c	3.372	3.340	3.363	3.315 [47, 49] ^a 3.314 [47] ^b 3.303 [6] ^c
ω_e, cm^{-1}	141	144	145	150 [49] ^a 144 [6] ^c 141 [50] ^d	111	115	115	119 [47,49] ^a 118 [6] ^c 117 [50] ^d
μ_e, D	10.9	10.7	11.3	10.8 [48, 49] ^a	11.6	11.5	12.1	11.6 [49] ^a
IP, eV	7.99	8.21	8.03	8.12 [48, 49] ^a	7.45	7.68	7.46	7.54 [47,49] ^a

Notes: $R_e(\text{Cs-X})$ is the equilibrium internuclear distance; ω_e is the normal mode frequency, μ_e is the dipole moment, IP is the ionization potential.

^aMicrowave spectrum; ^bElectron diffraction method; ^chigh level quantum chemical computation; ^dIR matrix isolation studies (Kr, Xe)

Table 2. Calculated and literature data of the Cs₂X₂ (X = Br or I) molecules

Property	Cs ₂ Br ₂				Cs ₂ I ₂			
	B3LYP5	B3P86	MP2	Reference	B3LYP5	B3P86	MP2	Reference
R _e (Cs-X)	3.373	3.332	3.326	3.356 [48] ^a 3.296 [6] ^b	3.621	3.578	3.578	3.572 [53] 3.511 [6] ^b
α _e (X-Cs-X)	90.5	90.3	89.1	85 [48] ^a 89.0 [6] ^b	94.0	93.7	92.6	92.4 [6] ^b
ω ₁ (A _g)	111	111	105	108 [50] 106 [6] ^b	83	87	105	95[50] 90 [53] 89 [6] ^b
ω ₂ (A _g)	41	43	45	41 [6] ^b	33	33	35	32 [6] ^b
ω ₃ (B _{1g})	83	87	93	94 [6] ^b	68	73	76	74 [6] ^b
ω ₄ (B _{1u})	29	29	31	28 [6] ^b	22	24	24	29 [54] ^d 21 [6] ^b
ω ₅ (B _{2u})	98	102	104	105 [6] ^b	81	85	86	88 [50] ^c 88 [6] ^b
ω ₆ (B _{3u})	100	104	108	110 [50] ^c 109 [6] ^b	79	83	84	76 [54] ^d 82 [6] ^b
I ₄	0.40	0.39	0.42		0.29	0.28	0.30	
I ₅	0.91	0.90	0.89		0.69	0.67	0.65	
I ₆	0.91	0.92	0.93		0.61	0.61	0.63	
Δ _r H°(0)	134.7	137.5	160.1	153.5 [55] 154.7 [6] ^f	128.6	131.1	153.8	150.9 [55] 147.1 [6] ^f
			150±5 ^e				143±13 ^e	

Notes: R_e(Cs-X) is the equilibrium internuclear distance, Å; α_e(X-Cs-X) is the valence angle in degrees; ω_i are the fundamental frequencies, cm⁻¹; I_i are the IR intensities, D²·amu⁻¹·Å⁻²; Δ_rH°(0) is the enthalpy of the dissociation reaction Cs₂X₂ = 2CsX, kJ·mol⁻¹.

^aElectron diffraction; ^bhigh level quantum chemical computation; ^cIR matrix isolation studies (Kr, Xe); ^dIR spectroscopy; ^eobtained by the MP4C method;

^fΔ_rH°(298 K) = 153.4 kJ·mol⁻¹ (Cs₂Br₂) and 145.6 kJ·mol⁻¹ (Cs₂I₂) obtained by high level quantum chemical computation in [6]; the enthalpy increments H°(298) – H°(0) of the monomer and dimer molecule used to recalculate Δ_rH°(298 K) into Δ_rH°(0) were taken from [55].

Therefore we expect the similar trend to appear in the properties of the ions considered further when the same level of computational method is applied.

The energies of dissociation reactions Δ_rE of Cs₂X₂ into CsX molecules have been calculated using different theoretical levels: B3LYP5, B3P86, MP2, MP2C, MP4, and MP4C. The enthalpies of reactions Δ_rH°(0) were obtained using the energies Δ_rE, and the zero-point vibration energy (ZPVE) correction Δε as given in following equations

$$\Delta_r H^\circ(0) = \Delta_r E + \Delta \varepsilon, \quad (1)$$

$$\Delta \varepsilon = \frac{1}{2}hc (\sum \omega_{i \text{ prod}} - \sum \omega_{i \text{ react}}), \quad (2)$$

where *h* is the Plank's constant, *c* is the speed of light in the free space, Σω_{*i* prod}, and Σω_{*i* react} are the sums of the vibration frequencies of the products and reactants, respectively.

The theoretical enthalpies of dissociations are compared with the reference values Δ_rH°(0) = 153.5 kJ·mol⁻¹ (Cs₂Br₂) and 150.9 kJ·mol⁻¹ (Cs₂I₂), accessed from the IVTANTHERMO Database [55]. Beside we take into consideration

here the results of a high level quantum chemical computation [6]: 154.7 kJ·mol⁻¹ (Cs₂Br₂) and 147.1 kJ·mol⁻¹ (Cs₂I₂). The comparison is presented in Figs. 2 a and 2 b where the experimental values from [55] are taken as a benchmark and the differences Δ between the theoretical and reference values are depicted by the bar diagrams. As one can see, B3LYP5 and B3P86 methods give underrated results for both dimeric species while MP2C and MP4 demonstrate rather good agreement. According to our highest level of computation, MP4C, Δ = -3.5 kJ·mol⁻¹ and -8.4 kJ·mol⁻¹ for Cs₂Br₂ and Cs₂I₂ respectively. Based on these results, and assuming a factor of 1.5, we estimated uncertainties to be ±5 kJ·mol⁻¹ and ±13 kJ·mol⁻¹ to the corresponding theoretical values of Δ_rH°(0) calculated by MP4C. It should be noted also that our result found by MP4C method for Cs₂Br₂ is in a good agreement with both reference data [55] and [6]. For Cs₂I₂ the agreement between the value 143±13 and experimental one, 150.9 [55], is worse, but within the uncertainties, there is no contradiction. If we take into account the data from [6] as a benchmark the agreement appeared to be better as seen in Fig. 2 c. Moreover the bar diagram in Fig. 2 c for cesium

iodide now looks alike to that of bromide (Fig. 2 a).

It is also worth to note here that the difference between the enthalpies of dissociation reactions $\Delta_r H^\circ(0)$ for Cs_2Br_2 and Cs_2I_2 is $7 \text{ kJ}\cdot\text{mol}^{-1}$ according to our results which agrees well with $\sim 8 \text{ kJ}\cdot\text{mol}^{-1}$ according to [6]. The last value seems to be more feasible than $2.6 \text{ kJ}\cdot\text{mol}^{-1}$ as it comes from [55]. The result of $\Delta_r H^\circ(0) = 164.1 \text{ kJ}\cdot\text{mol}^{-1}$ found for Cs_2I_2 on the base of the data $\Delta_r H^\circ(\text{CsI}, \text{g}, 298.15 \text{ K}) = -153.3 \pm 1.8$ and $\Delta_r H^\circ(\text{Cs}_2\text{I}_2, \text{g}, 298.15 \text{ K}) = -469.2 \pm 5 \text{ kJ}\cdot\text{mol}^{-1}$ reported recently by Roki et al. [7] is evidently higher than the enthalpy of dissociation of cesium bromide and therefore looks like overrated.

3.2 Geometrical Structure and Vibrational Spectra of the Cluster Ions

For the calculation of the properties of the cluster ions two methods; DFT (B3LYP5) and MP2 have been used. As a whole array of the data obtained for the neutral species, triatomic and pentaatomic, positive and negative ions demonstrates alike trends from DFT to MP2

levels, therefore we present hereafter the results found by more reliable MP2 method.

3.2.1 Triatomic ions Cs_2X^+ and CsX_2^-

Linear structures with $D_{\infty h}$ symmetry are proved to exist for the triatomic ions (Fig. 1 b, c). The properties such as equilibrium internuclear separations $R_e(\text{Cs-X})$, the frequencies of normal vibrations ω_i , and the intensities of vibrations in IR spectra I_i have been determined and given in Table 3.

It can be observed that internuclear separation $R_e(\text{Cs-X})$ increases by $\sim 0.08 \text{ \AA}$ from positive to negative ions for both species. Also an increase of internuclear distances by $\sim 0.25 \text{ \AA}$ has been featured across both positive and negative cesium bromide to cesium iodide. Clearly the increase of internuclear distance from positive to negative ions is due to an excess negative charge in the CsX_2^- ion, and from cesium bromide to cesium iodide is due to an extra shell. This increase in the internuclear distance corresponds to the decrease in the antisymmetric stretching frequency ω_2 : 138 cm^{-1} (Cs_2Br^+) to 109 cm^{-1} (Cs_2I^+); and 113 cm^{-1} (CsBr_2^-) to 98 cm^{-1} (CsI_2^-).

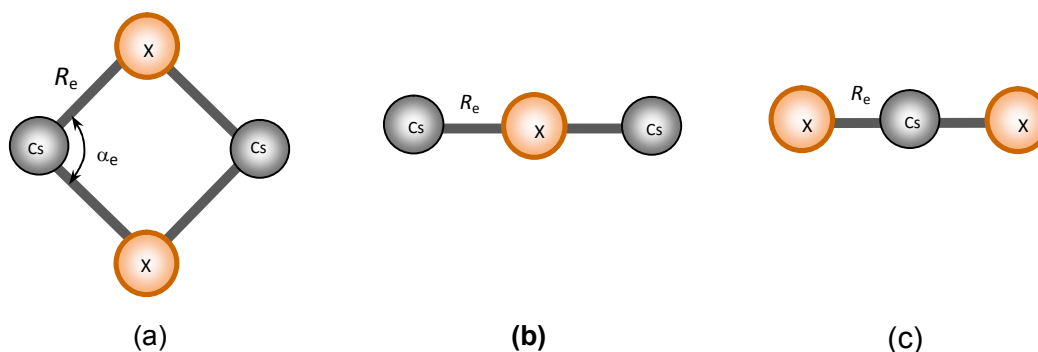


Fig. 1. Geometrical equilibrium structures of the dimer molecules Cs_2X_2 (a) and triatomic ions Cs_2X^+ (b) and CsX_2^- (c)

Table 3. Properties of the triatomic ions with linear configuration ($D_{\infty h}$), MP2 results

Property	Cs_2Br^+	CsBr_2^-	Cs_2I^+	CsI_2^-
$R_e(\text{Cs-X})$	3.264	3.345	3.509	3.590
$\omega_1 (\Sigma_g^+)$	70	88	65	65
$\omega_2 (\Sigma_u^+)$	138	113	109	98
$\omega_3 (\Pi_u)$	24	14	19	14
I_2	1.11	1.13	0.81	0.78
I_3	0.31	0.41	0.25	0.27

Notes: $R_e(\text{Cs-X})$ is the internuclear separation, \AA ; ω_i are the fundamental frequencies, cm^{-1} ; I_i are the IR intensities, $\text{D}^2\cdot\text{amu}^{-1}\cdot\text{\AA}^{-2}$

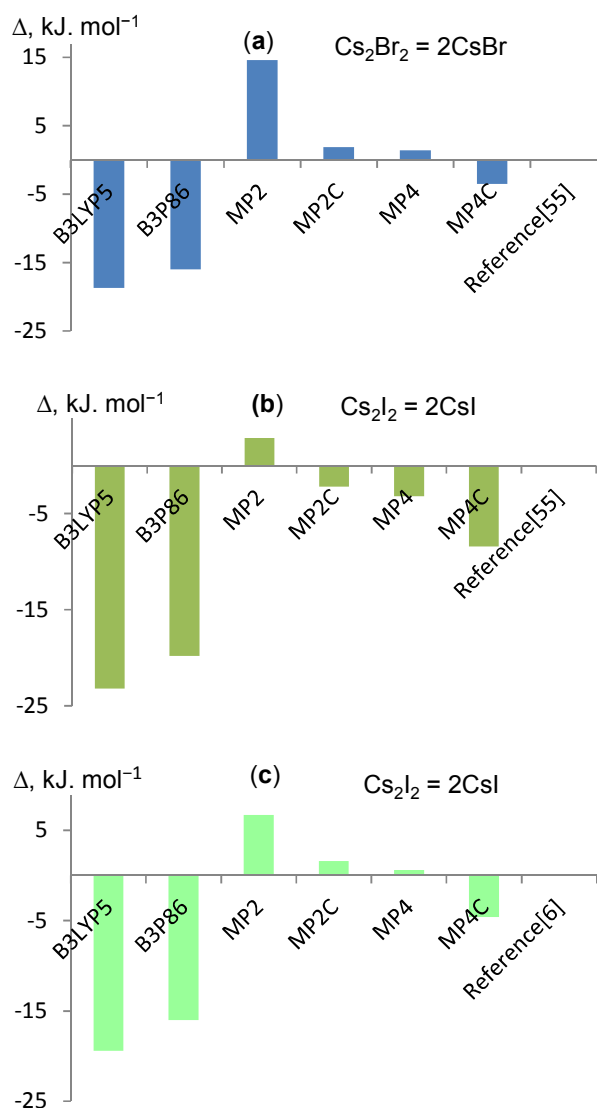


Fig. 2. Analysis of the calculated enthalpies of dissociation reactions $\Delta_r H^\circ(0)$ of the dimer molecules Cs_2Br_2 and Cs_2I_2 . Values of Δ are displayed versus the level of calculation; Δ is the difference between the theoretical $\Delta_r H^\circ(0)$ found by us and reference: (a) Cs_2Br_2 , reference [55]; (b) Cs_2I_2 , reference [55]; (c) Cs_2I_2 , reference [6]

3.2.2 Pentaatomic ions, Cs_3X_2^+ and Cs_2X_3^-

Three different possible configurations have been considered (Fig. 3): linear of $D_{\infty h}$ symmetry (I), planar cyclic (kite-shaped), C_{2v} (II), and bipyramidal, D_{3h} (III). For each structure, the geometrical parameters were optimized and fundamental frequencies were determined.

As concerns the linear configuration for the Cs_3Br_2^+ ion the imaginary frequencies have been revealed. The further optimization showed the

bent (V-shaped) structure of C_{2v} symmetry to exist with the valence angle $\alpha_e(\text{Br}-\text{Cs}-\text{Br}) = 144^\circ$ and practically without decrease in energy compared to the linear shape within the accuracy of optimization procedure. Other pentaatomic ions, Cs_2Br_3^- , Cs_3I_2^+ , and Cs_2I_3^- , were confirmed to be linear. Note these two equilibrium structures were obtained disregarding initial configuration started from: linear, bent or five-membered ring structures were converted during the optimization into V-shaped for Cs_3Br_2^+ or linear for other three ions. Here and hereafter we

call the isomer I as the ion of the bent (V-shaped) structure (C_{2v}) for the $Cs_3Br_2^+$ ion and linear ($D_{\infty h}$) for $Cs_2Br_3^-$, $Cs_3I_2^+$, and $Cs_2I_3^-$; their properties are given in Table 4. There are two different internuclear separations, terminal and bridge, which are denoted as $R_{et}(Cs-X)$ and $R_{eb}(Cs-X)$, respectively. From positive to negative ions of cesium bromide, there is a slight increase in the internuclear distance by 0.07 Å and 0.05 Å for $R_{et}(Cs-Br)$ and $R_{eb}(Cs-Br)$, respectively. The similar increase is observed for cesium iodide. Regarding terminal and bridge distances, for both ions the first one is shorter than the second, by ~0.16 Å for $Cs_3X_2^+$ and by ~0.13 Å for $Cs_2X_3^-$. In vibrational spectra of the ions with linear or V-shaped structure, several low deformational frequencies are observed, that gives evidence that these structures are floppy regarding to bending of the central moiety.

The isomer II, planar cyclic (C_{2v}), and isomer III, bipyramidal (D_{3h}), were also found to correspond to minima at the potential energy surface (PES). The optimized geometrical parameters were located and all calculated vibrational frequencies were confirmed to be real. Tables 5 and 6 report the properties of the ions $Cs_3X_2^+$ and $Cs_2X_3^-$ for cyclic and bipyramidal structures, their geometrical configurations are shown in Figs. 3 c, d, e, and f.

The cyclic structure is described by three different internuclear separations $Cs-X$, which are denoted as R_{e1} , R_{e2} , and R_{e3} , and two independent valence angles α_e and β_e . The internuclear distances of the negative ions are

slightly greater than those of positive ions correspondingly. The relative energy of the cyclic isomers with respect to the isomer I is $\Delta_r E_{iso} = E_{II} - E_I$ and for all four ions the values of $\Delta_r E_{iso}$ are negative and lie in the range between -8 and -12 $\text{kJ}\cdot\text{mol}^{-1}$. This result indicates that the cyclic isomer has lower energy on the PES than the isomer I and is more stable energetically. The vibrational spectra look alike for positive and negative ions both in frequencies and IR intensities.

The isomer III, that is of the bipyramidal shape, is specified by two parameters that are internuclear distance $R_e(Cs-X)$ and valence angle α_e . The internuclear distances for positive ions are slightly shorter than those for negative ions for cesium bromide or equal for iodide. We refer to the magnitudes of ionic radii of Cs^+ , Br^- , I^- ions. The bond angles at the vertices are almost the same and close to right angle. The corresponding vibrational frequencies of $Cs_3X_2^+$ and $Cs_2X_3^-$ ions are close to each other while the frequencies of positive ions are slightly larger than those of negative. The relative energy of bipyramidal isomer with respect to the isomer I is $\Delta_r E_{iso} = E_{III} - E_I$, the values of $\Delta_r E_{iso}$ are negative and in the range between -30 and -38 $\text{kJ}\cdot\text{mol}^{-1}$. Therefore the isomer III is more energetically stable than the linear one for $Cs_2Br_3^-$, $Cs_3I_2^+$, $Cs_2I_3^-$, and V-shaped for $Cs_3Br_2^+$. In addition the bipyramidal isomer has lower energy than cyclic one and thus appeared to be the most energetically stable among three alternative isomers.

Table 4. Properties of the pentaatomic ions, isomers I, MP2 results

Property	$Cs_3Br_2^+$ (C_{2v})	Property	$Cs_2Br_3^-$ ($D_{\infty h}$)	$Cs_3I_2^+$ ($D_{\infty h}$)	$Cs_2I_3^-$ ($D_{\infty h}$)
$R_{et}(Cs-X)$	3.216	$R_{et}(Cs-X)$	3.282	3.467	3.530
$R_{eb}(Cs-X)$	3.371	$R_{eb}(Cs-X)$	3.416	3.622	3.652
$\alpha_e(Br-Cs-Br)$	143.6				
$\beta_e(Cs-Br-Cs)$	179.5				
$\omega_1(A_1)$	138	$\omega_1(\sum_g^+)$	117	106	98
$\omega_2(A_1)$	51	$\omega_2(\sum_g^+)$	45	34	33
$\omega_3(A_1)$	25	$\omega_3(\sum_u^+)$	121	110	101
$\omega_4(A_1)$	8	$\omega_4(\sum_u^+)$	103	74	76
$\omega_5(A_2)$	23	$\omega_5(\Pi_g)$	10	13	14
$\omega_6(B_1)$	24	$\omega_6(\Pi_u)$	20	20	16
$\omega_7(B_2)$	137	$\omega_7(\Pi_u)$	3	8	10
$\omega_8(B_2)$	79				
$\omega_9(B_2)$	23				
μ_e	9.9				

Notes: $R_{et}(Cs-X)$ and $R_{eb}(Cs-X)$ are the terminal and bridge internuclear distances respectively, Å; $\alpha_e(Br-Cs-Br)$ and $\beta_e(Cs-Br-Cs)$ are the valence angles in degrees; ω_i are the fundamental frequencies, cm^{-1} ; μ_e is the dipole moment, D

Table 5. Properties of the pentaatomic ions with cyclic structure of C_{2v} symmetry (isomer II), MP2 results

Property	$Cs_3Br_2^+$	$Cs_2Br_3^-$	$Cs_3I_2^+$	$Cs_2I_3^-$
$R_{e1}(Cs-X)$	3.255	3.270	3.510	3.521
$R_{e2}(Cs-X)$	3.295	3.336	3.548	3.585
$R_{e3}(Cs-X)$	3.557	3.603	3.797	3.846
α_e	85.6	86.8	88.1	84.6
β_e	99.9	99.1	96.5	100.9
γ_e	135.5	136.3	136.4	135.1
$\Delta_r E_{iso}$	-8.4	-11.6	-9.2	-10.9
$\omega_1 (A_1)$	116	114	92	91
$\omega_2 (A_1)$	111	105	90	88
$\omega_3 (A_1)$	56	65	51	50
$\omega_4 (A_1)$	31	31	25	26
$\omega_5 (B_1)$	33	29	24	25
$\omega_6 (B_1)$	14	10	11	8
$\omega_7 (B_2)$	118	112	95	93
$\omega_8 (B_2)$	65	64	55	54
$\omega_9 (B_2)$	18	22	16	17
μ_e	9.4	6.7	10.8	7.8

Notes: $R_{e1}(Cs-X)$, $R_{e2}(Cs-X)$ and $R_{e3}(Cs-X)$ are internuclear distances, Å; α_e , β_e , and γ_e are the valence angles in degrees; $\Delta_r E_{iso} = E_{II} - E_I$ is the relative energy of the cyclic isomer, $\text{kJ}\cdot\text{mol}^{-1}$; ω_i are the normal mode frequencies, cm^{-1} ; μ_e is the dipole moment, D.

Table 6. Properties of the pentaatomic ions with bipyramidal structure of D_{3h} symmetry (isomer III), MP2 results

Property	$Cs_3Br_2^+$	$Cs_2Br_3^-$	$Cs_3I_2^+$	$Cs_2I_3^-$
$R_e(Cs-X)$	3.373	3.415	3.673	3.668
α_e	90.0	89.7	88.2	92.5
$\Delta_r E_{iso}$	-30.32	-38.48	-35.54	-38.14
$\omega_1 (A_1')$	111	104	86	84
$\omega_2 (A_1')$	52	54	49	43
$\omega_3 (A_2'')$	101	98	73	71
$\omega_4 (E')$	99	97	75	80
$\omega_5 (E')$	29	39	29	25
$\omega_6 (E')$	77	67	57	58

Notes: $R_e(Cs-X)$ is the internuclear distance, Å; α_e is the valence angle in degrees; $\Delta_r E_{iso} = E_{III} - E_I$ is the relative energy of the bipyramidal isomer, $\text{kJ}\cdot\text{mol}^{-1}$; ω_i are the normal mode frequencies, cm^{-1} .

3.3 Relative Concentration of Isomers

To examine the relative concentrations of isomers I, II, and III in saturated vapours over cesium bromide or iodide, thermodynamic calculations were performed. We considered the isomerization reactions $I \rightarrow II$ and $I \rightarrow III$. The relative concentrations x_i of the two isomers in equilibrium vapour was calculated using the following formula:

$$\Delta_r H^\circ(0) = T\Delta_r \Phi^\circ(T) - RT \ln x_i \quad (3)$$

where $\Delta_r H^\circ(0)$ is the enthalpy of the reaction; T is absolute temperature; $\Delta_r \Phi^\circ(T)$ is the change in the reduced Gibbs energy of the reaction, $\Phi^\circ(T) = -[H^\circ(T) - H^\circ(0) - TS^\circ(T)]/T$; $x_i = p_i/p_1$; p_i is the

partial pressure of the isomer II or III, and p_1 is the partial pressure of the isomer I. Hence here we have two ratios to be considered for each of the pentaatomic ions: $x_{II} = p_{II}/p_1$ and $x_{III} = p_{III}/p_1$. The enthalpies of the isomerization reactions $\Delta_r H^\circ(0)$ were evaluated using isomerization energies $\Delta_r E_{iso}$ and the ZPVE corrections $\Delta \epsilon$ by use of Eqs. (1) and (2); the energies $\Delta_r E_{iso}$ were calculated by MP4 method. The values of $\Delta_r \Phi^\circ(T)$ and other thermodynamic functions were calculated in the rigid rotator-harmonic oscillator approximation using the optimized coordinates and vibrational frequencies obtained in the MP2 calculations as the input parameters. The values of reduced Gibbs free energy and other thermodynamic functions are reported in the APPENDIX. The thermodynamic functions and

the relative concentration of the isomers were computed for the temperature range between 700 K and 1600 K related to the experimental condition. The results of calculations of energies and enthalpies of the isomerization reactions $\Delta_r H^\circ(0)$, ZPVE corrections $\Delta \varepsilon$, change in the reduced Gibbs free energies $\Delta_r \Phi^\circ(T)$, and relative concentration $x_i = p_i/p_1$ the isomers are reported in Table 7 for $T = 800$ K.

For each isomerization reaction considered the value of $\Delta_r H^\circ(0)$ is negative which means that the isomer in the right hand side of the reactions is more favorable by energy regarding the isomer I. Compared to the results found by the MP2 method the magnitudes of $\Delta_r H^\circ(0)$ by MP4 level are less and are in the range $\sim 20\text{--}30$ $\text{kJ}\cdot\text{mol}^{-1}$ for the bipyramidal isomer and $\sim 5\text{--}8$ $\text{kJ}\cdot\text{mol}^{-1}$ for cyclic isomer.

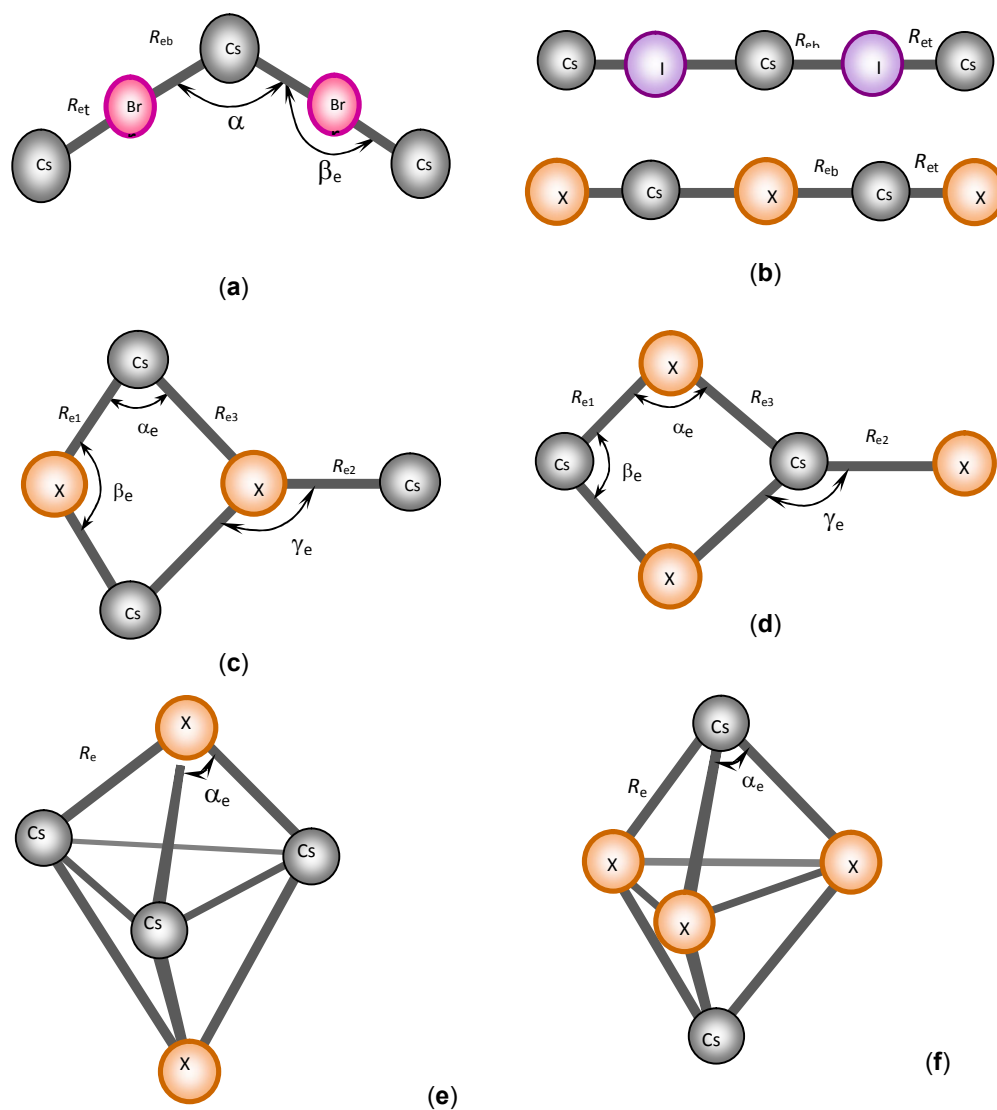


Fig. 3. Geometrical equilibrium structures of the isomers for pentaatomic ions: (a) V-shaped, C_{2v} , Cs_3Br_2^+ , (b) linear, $D_{\infty h}$, Cs_2Br_3^- , Cs_3I_2^+ , and Cs_2I_3^- , (c) planar cyclic, C_{2v} , Cs_3X_2^+ , (d) planar cyclic, C_{2v} , Cs_2X_3^- , (e) bipyramidal, D_{3h} , Cs_3X_2^+ , (f) bipyramidal, D_{3h} , Cs_2X_3^-

The value of x_i represents which isomer out of two is prevailing in the saturated vapour. One can see that $x_i < 1$ for all of the isomerization reactions that implies the isomer I is prevailing compared to the cyclic or bipyramidal. It is important to note here that for the ions Cs_3Br_2^+ , Cs_3I_2^+ , and Cs_2I_3^- the isomers I and II are found in comparable amount, but the bipyramidal one is not abundant. For the ion Cs_2Br_3^- the linear isomer is the most abundant compared with two others and actually only this one among the three exists.

The temperature dependence of the relative concentration x_i has been examined for the temperature range between 700 and 1600 K (Fig. 4). As is seen all relative concentrations of the isomers decrease with temperature increase. For the ion Cs_3Br_2^+ at 800 K, the concentration of cyclic isomer is 27% and decreases slowly to about 18% at 1500 K (Fig. 4 a). The concentrations of bipyramidal Cs_3Br_2^+ is 3% at 800 K and decreases to 0.7% at 1500 K. For the negative ion Cs_2Br_3^- the concentrations of both cyclic and bipyramidal are very low and decrease further with temperature rise (Fig. 4 b). For the ions Cs_3I_2^+ and Cs_2I_3^- , a very close appearance of the plots is observed in Figs 4 c, d. There is rather big amount of both cyclic and bipyramidal isomers at temperatures around 700–800 K, and then the relative concentrations are dropping down rapidly when the temperature rises still remaining essential for the cyclic species.

As the three isomers may occur in a comparable amount, the fraction w_i of each isomer out of three was found as well using the following equation:

$$w_i = \frac{p_i}{p_I + p_{II} + p_{III}}, \quad (4)$$

where p_i ($i = I, II, \text{ or } III$) represents the concentration of the isomer of interest. The fraction w_i was expressed through the ratio $x_i = p_i / p_I$ mentioned above:

$$w_i = \frac{x_i}{1 + x_{II} + x_{III}}. \quad (5)$$

The values of w_i at 800 K were found to be as follows: for Cs_3Br_2^+ are 0.77, 0.21 and 0.02; Cs_3I_2^+ are 0.66, 0.27 and 0.07 and Cs_2I_3^- are 0.70, 0.24 and 0.06 that is of linear, cyclic and bipyramid isomers, respectively. From these values, we can notice that the isomer I dominates for all ions, while the cyclic is less

abundant but still significant in its amount, and the fraction of the bipyramidal does not exceed 10%. Fig. 5 elucidates the influence of temperature on the fraction of isomers w_i . As it is seen raise in temperature increases the amount of linear isomer and decreases slowly that of cyclic isomers. For the bipyramid the fraction decreases rapidly as temperature elevates. Thus for all ions with temperature increase, the cyclic and bipyramidal isomers are decreasing in their content whereas isomer I is increasing and being predominant.

Concluding this section it is worth to emphasize the importance of the entropy factor on the relative content of the isomers. The effect of entropy and consequently in reduced Gibbs energy is appeared to be essential and prevailing over the energetic factor. In spite of the higher energetic stability of isomers II and III their relative amount is lower than of the isomer I. It is distinctly seen particularly for the bipyramidal isomer as its energy is lower by $\sim 30 \text{ kJ}\cdot\text{mol}^{-1}$ than that of the isomer I but its relative concentration is very small in saturated vapour at elevated temperatures. Therefore the considerable decrease in entropy of the isomerization reactions prevails over the energy factor and result in the predominance of the isomers I.

3.4 The Enthalpies of Dissociation Reactions and Enthalpies of Formation of Ions

In this section, we have examined the dissociation reactions of the cluster ions with elimination of CsX molecules. The energies of reactions $\Delta_r E$ have been calculated at different theoretical levels, B3LYP5, MP2, MP2C, MP4, MP4C, where in MP2C and MP4C the BSSE correction have been taken into account. The results are presented in Fig. 6. One can see the similar trend in values of $\Delta_r E$ with an enhancement of the theoretical level from B3LYP5 to MP4C i.e. the lowest values come from the B3LYP5 method, the highest ones from MP2 following by the further decreasing to the MP4C level. This trend is common either of tri- and pentaatomic ions. Also the distinct similarity may be observed for the same isomers of pentaatomic ions that is a slight oscillation of $\Delta_r E$ from MP2 to MP4C for isomer I and almost monotonic decrease for both cyclic and bipyramidal isomers. From these results the true value of $\Delta_r E$ comes when approaching the limit that we suppose is close to the MP4C result. The

latter appeared to be an intermediate between B3LYP5 and MP2 results. Regarding a certain pentaatomic ion, the change in $\Delta_r E$ is not the same for different isomers that is the change in $\Delta_r E$ from MP2 to MP4C is about $10 \text{ kJ}\cdot\text{mol}^{-1}$ for the isomers I or II, while that is $\sim 20 \text{ kJ}\cdot\text{mol}^{-1}$ for the isomers III.

This results in a small decrease of the isomerization energies from MP2 to MP4 and further to MP4C. The BSSE correction itself looks slightly different for three isomers of the same ion; that contributes to the error of computational scheme [46] and hence to the uncertainties of the theoretical values of the enthalpies of the dissociation reactions accepted here.

The values of $\Delta_r E$ obtained using the MP4C level were taken for calculation of the enthalpies of the reactions $\Delta_r H^\circ(0)$ by Eq. (1). The results on $\Delta_r E$, $\Delta_r H^\circ(0)$, ZPVE, and $\Delta_r H^\circ(0)$ are listed in Table 8. The reference thermodynamic data required for the calculations of the enthalpies of formation $\Delta_f H^\circ(0)$ of the cluster ions were retrieved from [55]. The uncertainties of the theoretical values were estimated on the base of the results for the dimer molecules Cs_2X_2 (section 3.1).

Regarding the positive and negative triatomic ions with the same halogen, Cs_2Br^+ and CsBr_2^- or Cs_2I^+ and CsI_2^- , have nearly equal enthalpies of reaction respectively, while for the ions with different halogens the values for bromides are higher by $7\text{--}10 \text{ kJ}\cdot\text{mol}^{-1}$ than for iodides. For all ions, the decrease in enthalpies of dissociation is observed from tri- to pentaatomic ions, so triatomic ions are apparently more stable against decomposition than pentaatomic ions.

For the pentaatomic ions the dissociation reactions are considered for each of three isomers. Comparing the isomers of the same shape for the positive and negative ions with the same halogen, one can see that the enthalpies are very close to each other, e.g. for Cs_3Br_2^+ (I) and Cs_2Br_3^- (I), $\Delta_r H^\circ(0) = 106$ and $108 \text{ kJ}\cdot\text{mol}^{-1}$, respectively or for Cs_3I_2^+ (III) and Cs_2I_3^- (III), $\Delta_r H^\circ(0) = 124$ and $125 \text{ kJ}\cdot\text{mol}^{-1}$, respectively. The bigger difference is observed for the bipyramidal isomers of Cs_3Br_2^+ and Cs_2Br_3^- , 123 and $135 \text{ kJ}\cdot\text{mol}^{-1}$ which is probably due to the smaller size of Br than Cs atom and hence the bipyramidal Cs_2Br_3^- ion with three Br atoms in the base has higher stability compared to Cs_3Br_2^+ with three Cs atoms in the base.

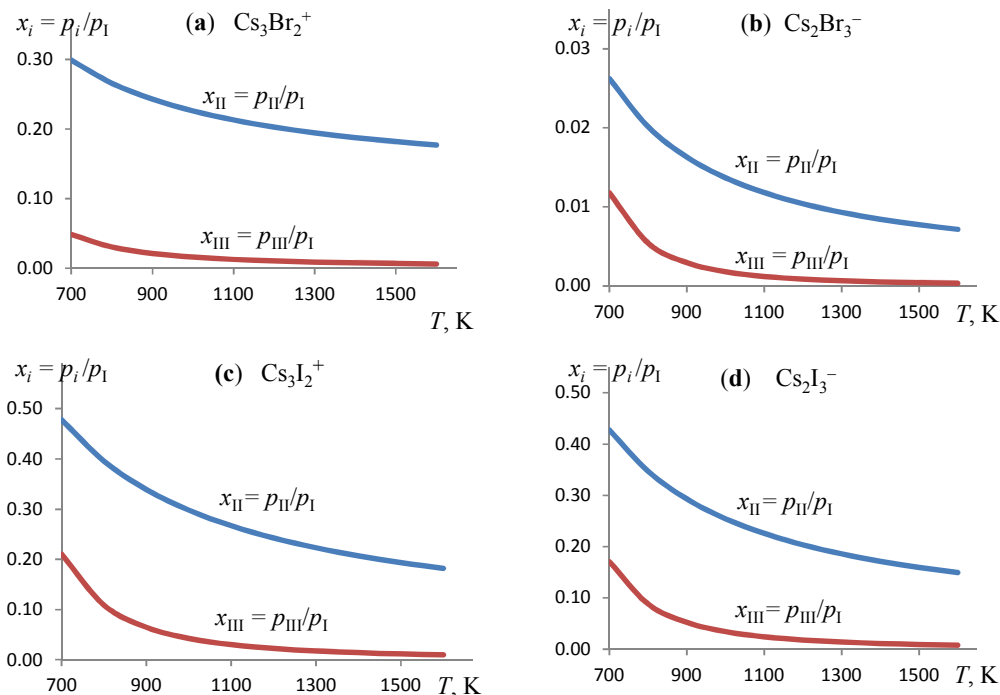


Fig. 4. Temperature dependence of the relative amount of pentaatomic ions isomers $x_i = p_i/p_1$ where $i = \text{II or III}$: (a) Cs_3Br_2^+ ; (b) Cs_2Br_3^- ; (c) Cs_3I_2^+ ; (d) Cs_2I_3^-

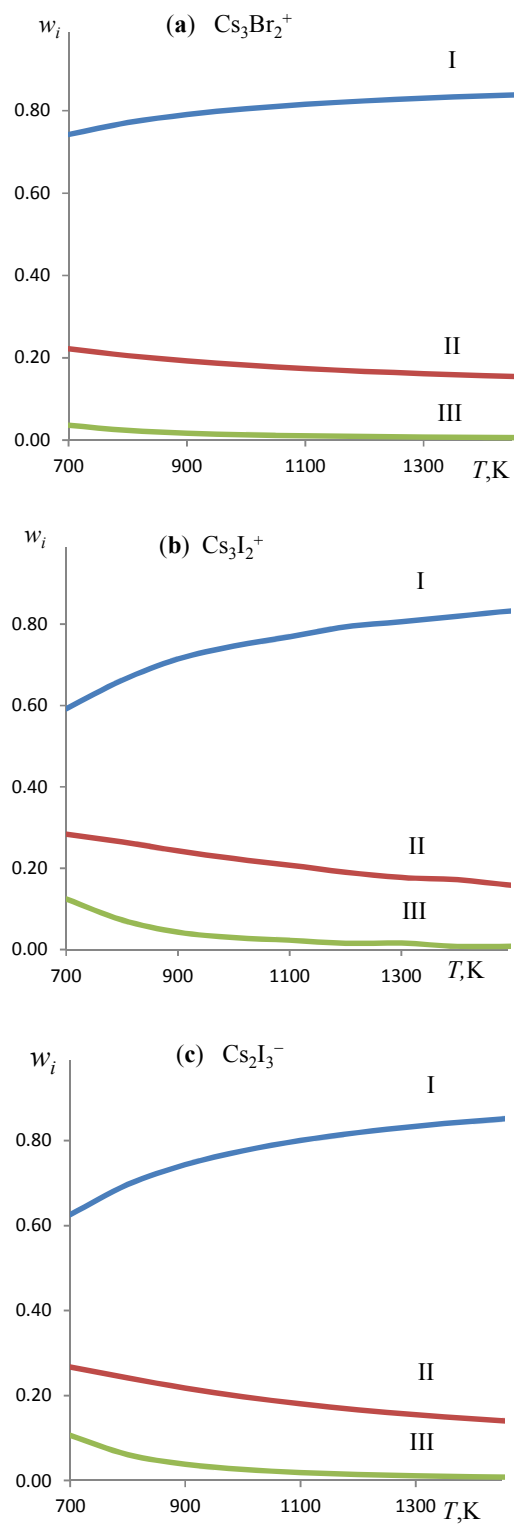


Fig. 5. The fractions w_i ($i = \text{I, II or III}$) of isomers versus temperature:
(a) Cs_3Br_2^+ ; (b) Cs_3I_2^+ ; (c) Cs_2I_3^-

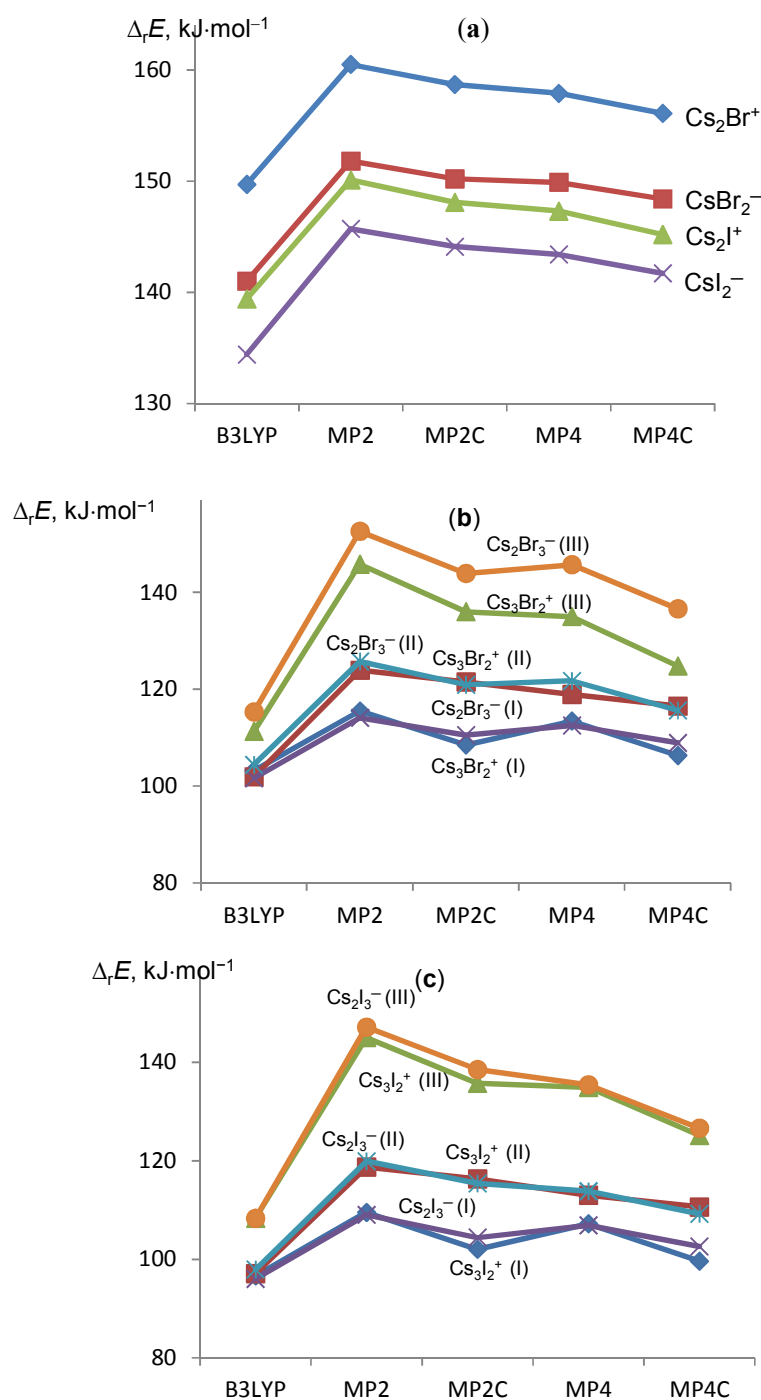


Fig. 6. The energies of dissociation reactions of the ions versus the level of calculation: (a) triatomic ions; (b) Cs_3Br_2^+ and Cs_2Br_3^- ; (c) Cs_3I_2^+ and Cs_2I_3^-

Comparing the bromides and corresponding iodides with the same shape and charge one can observe the higher values for bromides by 6–10 $\text{kJ}\cdot\text{mol}^{-1}$, e.g. for Cs_3Br_2^+ (I) and for Cs_3I_2^+ (I), $\Delta_r H^\circ(0) = 106$ and $99 \text{ kJ}\cdot\text{mol}^{-1}$, respectively or for

Cs_3Br_2^+ (III) and Cs_3I_2^+ (III), $\Delta_r H^\circ(0) = 135$ and $125 \text{ kJ}\cdot\text{mol}^{-1}$, respectively. The only one exclusion is observed for the enthalpies of dissociation of the bipyramidal ions Cs_3Br_2^+ and Cs_3I_2^+ ; 123 and $124 \text{ kJ}\cdot\text{mol}^{-1}$, as no decrease

from bromide to iodide is there. This result may be explained by a steric factor, the similar size of Cs and I atoms favours the Cs_3I_2^+ bipyramid compared to Cs_3Br_2^+ built of atoms of rather different size.

It is worth to remind here about the increase of stability of the isomers in the rank I–II–III; the enthalpy of dissociation of the isomer I is less by 6–11 $\text{kJ}\cdot\text{mol}^{-1}$ than of isomer II and 17–27 $\text{kJ}\cdot\text{mol}^{-1}$ compared to isomer III. The reason is that the isomers with compact shape are more stable against dissociation.

The experimental data are available in [24] for ions existing in vapour over cesium iodide where the ion molecular reactions were investigated by mass spectrometric method and the equilibrium constants K_p° for the heterophase reactions involving the tri- and pentaatomic cluster ions were measured. Using these constants we have computed the values of $\Delta_r H^\circ(0)$ by the formula:

$$\Delta_r H^\circ(0 \text{ K}) = -RT \ln K_p^\circ + T \Delta_r \Phi^\circ(T). \quad (6)$$

As an example, an ion molecular reaction for the positive triatomic ion may be expressed as follows:



where [CsI] corresponds to condensed phase. The equilibrium constant for this reaction is

$$K_p^\circ = \frac{p(\text{Cs}^+)}{p(\text{Cs}_2\text{I}^+)} = \frac{I(\text{Cs}^+)}{I(\text{Cs}_2\text{I}^+)} \sqrt{\frac{m(\text{Cs}^+)}{m(\text{Cs}_2\text{I}^+)}} \quad (8)$$

where I and m are ion currents and molecular mass of the ions, respectively. The thermodynamic functions of the ions Cs^+ and I^- , and [CsI] were taken from [55]. The enthalpies of heterophase reactions were converted into

enthalpies of gas phase reactions using the enthalpies of sublimation of CsI from [55]. The geometrical parameters and vibrational frequencies of the ions Cs_2I^+ , CsI_2^- , Cs_3I_2^+ , and Cs_2I_3^- needed for the calculation of the thermodynamic functions were taken from our MP2 results. The enthalpies of dissociation calculated through experimental data [24] are denoted as “based on experiment” hereafter and given in Table 8. As regards the pentaatomic ions, the existence of isomers had not been considered by Sidorova et al. [24]. In our work, as we have found the isomers may exist at a comparable amount, the fractions of the isomers, w_i ($i = \text{I, II, or III}$), are taken into account, that is the measured current is multiplied by the fraction, e.g. the ion current for isomer I is $I(\text{Cs}_3\text{I}_2^+, \text{I}) = I(\text{Cs}_2\text{I}_3^-)w_i$. The values of the ion currents obtained by this way have been used to calculate the equilibrium constant for each isomer and then the enthalpies of reactions $\Delta_r H^\circ(0)$ “based on experiment”. It is worth to note that for the pentaatomic ions only a few values of currents had been measured and no statistical treatment was done in [24].

As is seen in Table 8, for the triatomic ions, Cs_2I^+ and CsI_2^- , the theoretical magnitudes of $\Delta_r H^\circ(0)$ are in a good agreement with “based on experiment” values but underrated by ~ 5 $\text{kJ}\cdot\text{mol}^{-1}$. Similarly the theoretical values for the dimer molecules Cs_2I_2 are underrated compared to experimental data which is mentioned above. For the pentaatomic isomers the agreement in most cases is worse than for triatomic ions and the discrepancy between theoretical values and “based on experiment” approaches 13 $\text{kJ}\cdot\text{mol}^{-1}$. In addition, while the theoretical results demonstrate almost equal energetic stability of the positive Cs_3I_2^+ and negative Cs_2I_3^- ions of the same structure — 99 and 102 $\text{kJ}\cdot\text{mol}^{-1}$ for the

Table 7. The energies $\Delta_r E_{iso}$ and enthalpies $\Delta_r H^\circ(0)$ of the isomerization reactions, change in the reduced Gibbs free energies $\Delta_r \Phi^\circ(T)$, ZPVE corrections $\Delta \epsilon$, and relative abundances $x_i = p_i/p_i$ ($i = \text{II or III}$) of the isomers ($T = 800 \text{ K}$)

Isomerization reaction	$\Delta_r E_{iso}$ (MP4), $\text{kJ}\cdot\text{mol}^{-1}$	$\Delta \epsilon$, $\text{kJ}\cdot\text{mol}^{-1}$	$\Delta_r H^\circ(0)$, $\text{kJ}\cdot\text{mol}^{-1}$	$\Delta_r \Phi^\circ(T)$, $\text{J}\cdot\text{mol}^{-1}\cdot\text{K}^{-1}$	$x_i = p_i$ $/p_i$
$\text{Cs}_3\text{Br}_2^+ (\text{I}) = \text{Cs}_3\text{Br}_2^+ (\text{II})$	-5.4	0.32	-5.1	-17.4	0.27
$\text{Cs}_3\text{Br}_2^+ (\text{I}) = \text{Cs}_3\text{Br}_2^+ (\text{III})$	-21.6	0.96	-20.6	-54.8	0.03
$\text{Cs}_2\text{Br}_3^- (\text{I}) = \text{Cs}_2\text{Br}_3^- (\text{II})$	-9.2	0.60	-8.6	-43.2	0.02
$\text{Cs}_2\text{Br}_3^- (\text{I}) = \text{Cs}_2\text{Br}_3^- (\text{III})$	-33.2	1.21	-32.0	-83.4	0.005
$\text{Cs}_3\text{I}_2^+ (\text{I}) = \text{Cs}_3\text{I}_2^+ (\text{II})$	-5.8	0.32	-5.4	-14.5	0.40
$\text{Cs}_3\text{I}_2^+ (\text{I}) = \text{Cs}_3\text{I}_2^+ (\text{III})$	-27.7	0.74	-26.9	-52.1	0.11
$\text{Cs}_2\text{I}_3^- (\text{I}) = \text{Cs}_2\text{I}_3^- (\text{II})$	-7.0	0.39	-6.6	-17.0	0.35
$\text{Cs}_2\text{I}_3^- (\text{I}) = \text{Cs}_2\text{I}_3^- (\text{III})$	-28.5	0.82	-27.7	-54.8	0.09

Table 8. The dissociation reactions of the ions, energies $\Delta_r E$, enthalpies $\Delta_r H^\circ(0)$, and ZPVE corrections $\Delta \varepsilon$ of the reactions, and enthalpies of formation $\Delta_f H^\circ(0)$ of the ions; all values are in $\text{kJ}\cdot\text{mol}^{-1}$

No	Reaction	$\Delta_r E$	$\Delta \varepsilon$	$\Delta_r H^\circ(0)$		$\Delta_f H^\circ(0)$	
				Theoretical	Based on expt ^a	Theoretical	Based on expt ^a
1	$\text{Cs}_2\text{Br}^+ = \text{CsBr} + \text{Cs}^+$	156.1	-0.66	155±5		101±5	
2	$\text{CsBr}_2^- = \text{CsBr} + \text{CsBr}_2^-$	148.4	-0.50	148±5		-552±5	
3	$\text{Cs}_2\text{I}^+ = \text{CsI} + \text{Cs}^+$	145.2	-0.58	145±10	150 ± 5	160±10	155±5
4	$\text{CsI}_2^- = \text{CsI} + \text{I}^-$	141.7	-0.46	141±10	146 ± 5	-478±10	-483±5
5	$\text{Cs}_3\text{Br}_2^+(I) = \text{CsBr} + \text{Cs}_2\text{Br}^+$	106.3	-0.65	106±10		-202±10	
6	$\text{Cs}_3\text{Br}_2^+(II) = \text{CsBr} + \text{Cs}_2\text{Br}^+$	116.5	-0.96	116±10		-212±10	
7	$\text{Cs}_3\text{Br}_2^+(III) = \text{CsBr} + \text{Cs}_2\text{Br}^+$	124.8	-1.60	123±10		-219±10	
8	$\text{Cs}_2\text{Br}_3^-(I) = \text{CsBr} + \text{CsBr}_2^-$	108.9	-0.47	108±10		-858±10	
9	$\text{Cs}_2\text{Br}_3^-(II) = \text{CsBr} + \text{CsBr}_2^-$	115.6	-0.47	115±10		-864 ± 10	
10	$\text{Cs}_2\text{Br}_3^-(III) = \text{CsBr} + \text{CsBr}_2^-$	136.6	-1.67	135±10		-884 ± 10	
11	$\text{Cs}_3\text{I}_2^+(I) = \text{CsI} + \text{Cs}_2\text{I}^+$	99.6	-0.47	99±15	108±12	-88±15	-102±12
12	$\text{Cs}_3\text{I}_2^+(II) = \text{CsI} + \text{Cs}_2\text{I}^+$	110.6	-0.79	110±15	114±12	-99±15	-108±12
13	$\text{Cs}_3\text{I}_2^+(III) = \text{CsI} + \text{Cs}_2\text{I}^+$	125.1	-1.21	124±15	135±12	-113±15	-129±12
14	$\text{Cs}_2\text{I}_3^-(I) = \text{CsI} + \text{CsI}_2^-$	102.6	-0.48	102±15	114±12	-729±15	-746±12
15	$\text{Cs}_2\text{I}_3^-(II) = \text{CsI} + \text{CsI}_2^-$	109.2	-0.87	108±15	118±12	-735±15	-750±12
16	$\text{Cs}_2\text{I}_3^-(III) = \text{CsI} + \text{CsI}_2^-$	126.6	-1.30	125±15	138±12	-757±15	-770±12

^aThe values $\Delta_f H^\circ(0)$ "based on experiment" were determined by us on the base of the equilibrium constants from [24] and our thermodynamic functions. The uncertainties for the triatomic ions were taken from [24] and for pentaatomic estimated by us. In the original work by Sidorova et al. [24], the enthalpies of the dissociation reactions (3) and (4) were 151.0 ± 5.4 and $151.4 \pm 5.4 \text{ kJ}\cdot\text{mol}^{-1}$, respectively. These values were found on the basis of the experimental equilibrium constants and estimated geometrical parameters and vibrational frequencies of the ions

isomer I, 110 and $108 \text{ kJ}\cdot\text{mol}^{-1}$ for isomer II, 124 and $125 \text{ kJ}\cdot\text{mol}^{-1}$ for III — however the data "based on experiment" show a small systematic increase in stability by $3\text{--}6 \text{ kJ}\cdot\text{mol}^{-1}$ from the positive to negative ions correspondingly. Therefore when we consider the different trends, i.e. from bromides to iodides, from triatomic to pentaatomic, from positive to negative, it is indicative that the experimental values for the cesium iodide species seem to be slightly overrated. Nevertheless, within the uncertainty limits, the theoretical and "based on experiment" values of $\Delta_f H^\circ(0)$ are in satisfactory agreement and there is no crucial contradiction between them. The similar agreement is seen for the enthalpies of formation of the ions $\Delta_f H^\circ(0)$ presented in Table 8.

4. CONCLUSION

The DFT (B3LYP5) and MP2 methods have been used to calculate geometrical parameters and vibrational frequencies of different cluster ions Cs_2X^+ , Cs_3X_2^+ , CsX_2^- , and Cs_2X_3^- (X = Br or I) existing in saturated vapours over cesium bromide and iodide. The results obtained by DFT and MP2 methods do not contradict each other and literature data as well. Nevertheless the MP2 method yields preferable results.

For the pentaatomic ions Cs_3X_2^+ and Cs_2X_3^- different isomers of linear, planar cyclic, bipyramidal, and V-shaped were proved to exist in considerable fractions. The properties of the species with the similar structure look alike for positive and negative ions both in vibrational spectra and energetic stability. In spite of the highest energetic stability of the bipyramidal isomer its relative concentration is appeared to be small in saturated vapours at elevated temperatures.

Regarding the enthalpies of dissociation reactions of the dimer molecules and ions, $\Delta_r H^\circ(0)$, the DFT (B3LYP5 and B3P86) methods bring rather underrated values compared with experimental data available. The higher level of calculations MP4C allowed us to approach more reliable results and come to better agreement with the literature data. Still as concerns cesium iodide species — the dimer molecule and ions — detailed analysis of the theoretical and experimental data shows that the experimental values of $\Delta_r H^\circ(0)$ seem to be somehow overrated and it would be desirable to refine them applying advanced experimental techniques.

ACKNOWLEDGEMENT

The authors are grateful to the Nelson Mandela African Institution of Science and Technology (NM-AIST) for the sponsorship. We are also acknowledge the precious assistance and service by the School of Computational and Communication Sciences and Engineering (CoCSE) of NM-AIST and Mr. Adam Mawenya personally.

COMPETING INTERESTS

Authors have declared that no competing interests exist.

REFERENCES

1. Khanna SN, Jena P. Atomic clusters: Building blocks for a class of solids. *Phys Rev B*. 1995;51(19):13705-13716.
2. Khanna S, Jena P. Assembling crystals from clusters. *Phys Rev Letters*. 1993; 71(1):208-301.
3. Rao B, Khanna S, Jena P. Designing new materials using atomic clusters. *J Cluster Science*. 1999;10(4):477-491.
4. Castleman Jr A, Khanna S. Clusters, superatoms, and building blocks of new materials. *J Phys Chem C*. 2009; 113(7):2664-2675.
5. Lennart D, Kjell J. Specific features of cesium chemistry and physics affecting reactor accident source term predictions; 1994. Organisation for Economic Co-Operation and Development-Nuclear Energy Agency, Committee on the safety of nuclear installations-OECD/NEA/CSNI, Le Seine Saint-Germain, 12 boulevard des Iles, F-92130 Issy-les-Moulineaux (France).
6. Badawi M, Xerri B, Canneaux S, Cantrel L, Louis F. Molecular structures and thermodynamic properties of 12 gaseous cesium-containing species of nuclear safety interest: Cs₂, CsH, CsO, Cs₂O, CsX, and Cs₂X₂ (X = OH, Cl, Br, and I). *J Nuclear Materials*. 2012;420(1):452-462.
7. Roki FZ, Ohnet MN, Fillet S, Chatillon C, Nuta I. Critical assessment of thermodynamic properties of CsI solid, liquid and gas phases. *J Chem Thermodynamics*. 2014;70:46-72.
8. Roki F, Ohnet M, Fillet S, Chatillon C, Nuta I. Knudsen cell mass spectrometric study of the Cs₂I/OH (g) molecule thermodynamics. *J Chem Thermodynamics*. 2013;65:247-264.
9. Povinec PP, Aoyama M, Biddulph D, Breier R, Buesseler K, Chang C, Golser R, Hou X, Jeřkovský M, Jull A. Cesium, iodine and tritium in NW Pacific waters—a comparison of the Fukushima impact with global fallout. *Biogeosciences Discussions*. 2013;10(4):5481-5496.
10. Sarkas HW, Kidder LH, Bowen KH. Photoelectron spectroscopy of color centers in negatively charged cesium iodide nanocrystals. *J Chem Phys*. 1995; 102(1):57-66.
11. Alexandrova AN, Boldyrev AI, Fu YJ, Yang X, Wang XB, Wang LS. Structure of the Na_xCl⁻_{x+1} (x = 1–4) clusters via ab initio genetic algorithm and photoelectron spectroscopy. *J Chem Phys*. 2004; 121(12):5709-5719.
12. Huh S, Lee G. Mass spectrometric study of negative, positive and mixed KI cluster ions by using fast Xe atom bombardment. *J Korean Phys Society*. 2001;38(2):107-110.
13. Castleman A, Bowen K. Clusters: Structure, energetics and dynamics of intermediate states of matter. *J Phys Chem*. 1996;100(31):12911-12944.
14. Aguado A. An ab initio study of the structures and relative stabilities of doubly charged [(NaCl)_m(Na)₂]²⁺ cluster ions. *J Phys Chem B*. 2001;105(14):2761-2765.
15. Yang Y, Bloomfield L, Jin C, Wang L, Smalley R. Ultraviolet photoelectron spectroscopy and photofragmentation studies of excess electrons in potassium iodide cluster anions. *J Chem Phys*. 1992; 96(4):2453-2459.
16. Anil K, Kandalam PJ, Xiang L, Soren ME, Bowen KH. Photoelectron spectroscopy and theoretical studies of [Co_m(pyrene)_n]⁻ (m = 1,2 and n = 1,2) complexes. *J Chem Phys*. 2008;129:134308-134318.
17. Galhena AS, Jones CM, Wysocki VH. Influence of cluster size and ion activation method on the dissociation of cesium iodide clusters. *Inter J Mass Spectrometry*. 2009;287(1):105-113.
18. Bloomfield LA, Conover CWS, Yang YA, Twu YJ, Phillips NG. Experimental and theoretical studies of the structure of alkali halide clusters. *Atoms, Molecules and Clusters*. 1991;20:93-96.
19. Chupka WA. Dissociation energies of some gaseous alkali halide complex ions

- and the hydrated ion $K(H_2O)^+$. *J Chem Phys.* 1959;10:458-465.
20. Gusarov AV. Equilibrium ionization in vapors of inorganic compounds and the thermodynamic properties of ions. *Chem Sciences Doctoral Dissertation*; 1986. Moscow.
 21. Kudin LS, Burdukovskaya GG, Krasnov KS, Vorob'ev OV. Mass spectrometric study of the ionic composition of saturated potassium chloride vapour. Enthalpies of formation of the K_2Cl^+ , $K_3Cl_2^+$, KCl_2^- , and $K_2Cl_3^-$ ions. *Russ J Phys Chem.* 1990; 64:484-489.
 22. Motalov VB, Pogrebnoi AM, Kudin LS. Molecular and ionic associates in vapor over rubidium chloride. *Russ J Phys Chem.* 2001;75:407-1412.
 23. Pogrebnoi AM, Kudin LS, Kuznetsov AY. Enthalpies of formation of the ions present in the saturated vapor over cesium chloride. *Russ J Phys Chem.* 2000; 74:1728-1730.
 24. Sidorova I, Gusarov A, Gorokhov L. Ion-molecule equilibria in the vapors over cesium iodide and sodium fluoride. *Int J Mass Spectrom and Ion Phys.* 1979; 31(4):367-372.
 25. Dunaev AM, Kudin LS, Butman MF, Motalov VB. Alkali halide work function determination by Knudsen effusion mass spectrometry. *Electrochemical Society Transactions.* 2013;46(1):251-258.
 26. Castleman A, Jena P. Clusters: A bridge between disciplines. *Proceedings of the National Academy of Sciences.* 2006; 103(28):10552-10553.
 27. Pogrebnaya T, Pogrebnoi A, Kudin L. Calculation of the thermodynamic characteristics of ions in vapor over sodium fluoride. *Russ J Phys Chem A.* 2008;82(1):75-82.
 28. Pogrebnaya T, Pogrebnoi A, Kudin L. Structural and thermodynamic characteristics of ionic associates in vapors over sodium bromide and iodide. *J Struct Chem.* 2010;51(2):231-237.
 29. Pogrebnaya TP, Hishamunda JB, Girabawe C, Pogrebnoi AM. Theoretical study of structure, vibration spectra and thermodynamic properties of cluster ions in vapors over potassium, rubidium and cesium chlorides. *Chem Sustainable Dev.* Springer. 2012;353-366.
 30. Pogrebnaya T, Pogrebnoi A, Kudin L. Theoretical study of the structure and stability of the Na_2Cl^+ , $NaCl_2^-$, $Na_3Cl_2^+$ and $Na_2Cl_3^-$ ions. *J Struct Chem.* 2007; 48(6):987-995.
 31. Butman M, Kudin L, Smirnov A, Munir Z. Mass spectrometric study of the molecular and ionic sublimation of cesium iodide single crystals. *Int J Mass Spectrom.* 2000; 202(1):121-137.
 32. Wang YL, Wang XB, Xing XP, Wei F, Li J, Wang LS. Photoelectron imaging and spectroscopy of Ml_2^- ($M= Cs, Cu, Au$): Evolution from ionic to covalent bonding. *J Phys Chem A.* 2010;114(42):11244-11251.
 33. Parks E, Inoue M, Wexler S. Collision induced dissociation of CsI and Cs_2I_2 to ion pairs by Kr, Xe, and SF_6 . *J Chem Phys.* 1982;76(3):1357-1379.
 34. Schmidt MW, Baldrige KK, Boatz JA, Elbert ST, Gordon MS, Jensen JH, Koseki S, Matsunaga N, Nguyen KA, Su S, Windus TL, Dupuis M, Montgomery JA. General atomic and molecular electronic structure system. *J Comput. Chem.* 1993;14:1347-1363. DOI: 10.1002/jcc.540141112.
 35. Granovsky AA. Firefly version 8.0.0, www; 2012. (Accessed 15 March 2015) Available:<http://classic.chem.msu.su/gran/firefly/index.html>
 36. Lee C, Yang W, Parr RG. Development of the Colle-Salvetti correlation-energy formula into a functional of the electron density. *Phys Rev B.* 1988;37(2):785.
 37. Becke AD. Density-functional thermochemistry. III. The role of exact exchange. *J Chem Phys.* 1993;98(7):5648-5652.
 38. Perdew JP, Zunger A. Self-interaction correction to density-functional approximations for many-electron systems. *Phys Rev B.* 1981;23(10):5048.
 39. Perdew JP. Density-functional approximation for the correlation energy of the inhomogeneous electron gas. *Phys Rev B.* 1986;33(12):8822.
 40. Leininger T, Nicklass A, Küchle W, Stoll H, Dolg M, Bergner A. The accuracy of the pseudopotential approximation: Non-frozen-core effects for spectroscopic constants of alkali fluorides XF ($X= K, Rb, Cs$). *Chem Phys Letters.* 1996;255(4):274-280.
 41. Martin JM, Sundermann A. Correlation consistent valence basis sets for use with the Stuttgart–Dresden–Bonn relativistic effective core potentials: The atoms Ga–Kr and In–Xe. *J Chem Phys.* 2001; 114(8):3408-3420.

42. Basis set library EMSL (The Environmental Molecular Sciences Laboratory, U.S.). Accessed 10 March 2015. Available: <https://bse.pnl.gov/bse/portal>
43. Schuchardt KL, Didier BT, Elsethagen T, Sun L, Gurumoorthi V, Chase J, Li J, Windus TL. Basis set exchange: a community database for computational sciences. *J Chem Information and Modeling*. 2007;47(3):1045-1052.
44. Feller D. The role of databases in support of computational chemistry calculations. *J Comput Chem*. 1996;17(13):1571-1586.
45. Boys SF, Bernardi F. The calculation of small molecular interactions by the differences of separate total energies. Some procedures with reduced errors. *Mol. Phys*. 1970;19:553-556.
46. Solomonik VG, Smirnov AN, Mileev MA. Structure, vibrational spectra and energetic stability of LnX_4^- ($\text{Ln} = \text{La}, \text{Lu}; \text{X} = \text{F}, \text{Cl}, \text{Br}, \text{I}$) ions. *Koord Khim*. 2005;31:218-228.
47. Hartley J, Fink M. An electron diffraction study of alkali iodide vapors. *J Chem Phys*. 1988;89(10):6053-6057.
48. Hartley J, Fink M. An electron diffraction study of alkali bromide vapors. *J Chem Phys*. 1987;87(9):5477-5482.
49. Huber K, Herzberg G. Constants of diatomic molecules (data prepared by JW Gallagher and RD Johnson, III) in NIST Chemistry WebBook, NIST Standard Reference Database Number 69, eds. PJ Linstrom and WG Mallard; 2001. Accessed 10 March 2015. Available: webbook.nist.gov
50. Groen CP, Kovács A. Matrix-isolation FT-IR study of $(\text{CsBr})_n$ and $(\text{CsI})_n$ ($n = 1-3$). *Vibrational Spectroscopy*. 2010;54(1):30-34.
51. Hargittai M. Molecular structure of metal halides. *Chem Rev*. 2000;100(6):2233-2302.
52. Dickey RP, Maurice D, Cave RJ, Mawhorter R. A theoretical investigation of the geometries, vibrational frequencies, and binding energies of several alkali halide dimers. *J Chem Phys*. 1993; 98(3):2182-2190.
53. Cordfunke EHP, Konings RJM. Thermochemical data for reactor materials and fission products. Elsevier, Amsterdam; 1990.
54. Konings R, Booij A, Cordfunke E. High-temperature infrared study of the vaporization of CsI , CdI_2 and Cs_2CdI_4 . *Vibrational Spectroscopy*. 1991;2(4):251-255.
55. Gurvich LV, Yungman VS, Bergman GA, Veitz IV, Gusarov AV, Iorish VS, Leonidov VY, Medvedev VA, Belov GV, Aristova NM, Gorokhov LN, Dorofeeva OV, Ezhov YS, Efimov ME, Krivosheya NS, Nazarenko I, Osina EL, Ryabova VG, Tolmach PI, Chandamirova NE, Shenyavskaya EA. Thermodynamic properties of individual substances. IVTANTHERMO for Windows database on thermodynamic properties of individual substances and thermodynamic modeling software, Version 3.0; 1992-2000. Glushko Thermocenter of RAS, Moscow.

APPENDIX

Thermodynamic Functions of the Cluster Ions

The thermodynamic functions of cluster ions Cs_2X^+ , CsX_2^- , Cs_3X_2^+ , Cs_2X_3^- ($\text{X} = \text{Br}, \text{I}$) used in calculations are given in Tables A₁–A₈ and B₁–B₈ for cesium bromide and cesium iodide, respectively: Φ° is the reduced Gibbs free energy; S° is entropy; and $H^\circ(T) - H^\circ(0)$ is the enthalpy increment. The values of Φ° , and S° are given in $\text{J}\cdot\text{mol}^{-1}\cdot\text{K}^{-1}$, and $H^\circ(T) - H^\circ(0)$ in $\text{kJ}\cdot\text{mol}^{-1}$; absolute temperature T in kelvins.

Table A₁. Thermodynamic functions of Cs_2Br^+

T	Φ°	S°	$H^\circ(T) - H^\circ(0)$
298.15	295.239	352.864	17.181
700	345.678	405.922	42.171
800	353.739	414.240	48.401
900	360.877	421.579	54.631
1000	367.282	428.145	60.863
1100	373.089	434.085	67.096
1200	378.401	439.508	73.329
1300	383.296	444.498	79.563
1400	387.835	449.118	85.796
1500	392.065	453.419	92.031
1600	396.027	457.442	98.265

Table A₂. Thermodynamic functions of CsBr_2^-

T	Φ°	S°	$H^\circ(T) - H^\circ(0)$
298.15	297.551	355.651	17.323
700	348.273	408.736	42.324
800	356.363	417.056	48.555
900	363.522	424.396	54.786
1000	369.943	430.962	61.019
1100	375.765	436.903	67.252
1200	381.089	442.327	73.485
1300	385.994	447.317	79.719
1400	390.542	451.937	85.954
1500	394.779	456.238	92.188
1600	398.748	460.262	98.423

Table A₃. Thermodynamic functions of Cs_3Br_2^+ , isomer I (V-shaped)

T	Φ°	S°	$H^\circ(T) - H^\circ(0)$
298.15	435.304	533.967	29.416
700	522.016	625.898	66.897
800	535.923	640.315	76.862
900	548.242	653.034	86.830
1000	559.300	664.414	96.800
1100	569.332	674.710	106.770
1200	578.510	684.110	116.742
1300	586.970	692.758	126.715
1400	594.817	700.766	136.689
1500	602.131	708.221	146.663
1600	608.983	715.195	156.637

Table A₄. Thermodynamic functions of Cs₂Br₃⁻, isomer I (linear)

<i>T</i>	Φ°	<i>S</i> [°]	<i>H</i> [°] (<i>T</i>) – <i>H</i> [°] (0)
298.15	453.6812	557.533	30.963
700	544.552	653.058	75.954
800	559.072	668.032	87.168
900	571.926	681.242	98.384
1000	583.459	693.061	109.602
1100	593.917	703.754	120.821
1200	603.483	713.517	132.041
1300	612.296	722.498	143.262
1400	620.469	730.814	154.483
1500	628.087	738.556	165.704
1600	635.220	745.799	176.926

Table A₅. Thermodynamic functions of Cs₃Br₂⁺, isomer II (cyclic)

<i>T</i>	Φ°	<i>S</i> [°]	<i>H</i> [°] (<i>T</i>) – <i>H</i> [°] (0)
298.15	418.579	516.190	29.103
700	504.685	608.116	3290.293
800	518.535	622.532	1388.692
900	530.811	635.252	842.065
1000	541.834	646.632	592.264
1100	551.836	656.927	451.532
1200	560.990	666.327	362.226
1300	569.430	674.975	300.905
1400	577.259	682.983	256.380
1500	584.559	690.438	222.694
1600	591.397	697.412	196.462

Table A₆. Thermodynamic functions of Cs₂Br₃⁻, isomer II (cyclic)

<i>T</i>	Φ°	<i>S</i> [°]	<i>H</i> [°] (<i>T</i>) – <i>H</i> [°] (0)
298.15	415.791	513.565	29.151
700	501.997	605.507	72.457
800	515.857	619.924	83.254
900	528.141	632.644	94.053
1000	539.170	644.024	104.854
1100	549.177	654.320	115.657
1200	558.336	663.720	126.461
1300	566.780	672.368	137.265
1400	574.612	680.376	148.070
1500	581.914	687.831	158.876
1600	588.754	694.805	169.682

Table A₇. Thermodynamic functions of Cs₃Br₂⁺, isomer III (bipyramidal)

<i>T</i>	Φ°	<i>S</i> [°]	<i>H</i> [°] (<i>T</i>) – <i>H</i> [°] (0)
298.15	382.493	478.083	28.500
700	467.417	569.957	71.778
800	481.156	584.371	82.572
900	493.344	597.088	93.369
1000	504.298	608.467	104.169
1100	514.244	618.762	114.970
1200	523.350	628.161	125.773
1300	531.750	636.808	136.576
1400	539.543	644.815	147.381
1500	546.813	652.270	158.185
1600	553.625	659.244	168.991

Table A₈. Thermodynamic functions of Cs₂Br₃⁻, isomer III (bipyramidal)

<i>T</i>	Φ°	<i>S</i> [°]	<i>H</i> [°] (<i>T</i>) – <i>H</i> [°] (0)
298.150	376.844	472.659	28.567
700	461.910	564.564	71.858
800	475.663	578.979	82.653
900	487.863	591.698	93.451
1000	498.825	603.077	104.252
1100	508.778	613.373	115.054
1200	517.891	622.772	125.857
1300	526.296	631.420	136.661
1400	534.095	639.427	147.465
1500	541.368	646.882	158.271
1600	548.184	653.856	169.076

Table B₁. Thermodynamic functions of Cs₂I⁺

<i>T</i>	Φ°	<i>S</i> [°]	<i>H</i> [°] (<i>T</i>) – <i>H</i> [°] (0)
298.15	303.678	362.054	17.405
700	354.570	415.166	42.417
800	362.676	423.487	48.649
900	369.848	430.827	54.881
1000	376.280	437.395	61.115
1100	382.110	443.336	67.348
1200	387.442	448.760	73.582
1300	392.353	453.750	79.817
1400	396.906	458.371	86.051
1500	401.148	462.672	92.286
1600	405.121	466.696	98.521

Table B₂. Thermodynamic functions of CsI₂⁻

<i>T</i>	Φ°	<i>S</i> [°]	<i>H</i> [°] (<i>T</i>) – <i>H</i> [°] (0)
298.15	309.246	368.052	17.533
700	360.392	421.184	42.554
800	368.523	429.506	48.787
900	375.715	436.848	55.020
1000	382.163	443.416	61.254
1100	388.006	449.358	67.488
1200	393.347	454.782	73.722
1300	398.267	459.772	79.957
1400	402.828	464.393	86.191
1500	407.078	468.695	92.426
1600	411.056	472.719	98.661

Table B₃. Thermodynamic functions of Cs₃I₂⁺, isomer I (linear)

<i>T</i>	Φ°	<i>S</i> [°]	<i>H</i> [°] (<i>T</i>) – <i>H</i> [°] (0)
298.150	446.083	550.685	31.187
700	537.413	646.280	76.207
800	551.977	661.257	87.424
900	564.868	674.470	98.642
1000	576.429	686.291	109.862
1100	586.911	696.986	121.082
1200	596.497	706.749	132.303
1300	605.327	715.731	143.525
1400	613.514	724.048	154.747
1500	621.145	731.791	165.969
1600	628.288	739.033	177.192

Table B₄. Thermodynamic functions of Cs₂I₃⁻, isomer I (linear)

<i>T</i>	Φ°	<i>S</i> [°]	<i>H</i> [°] (<i>T</i>) – <i>H</i> [°] (0)
298.15	445.83	550.755	31.283
700	537.355	646.374	76.313
800	551.940	661.353	87.531
900	564.845	674.567	98.750
1000	576.418	686.388	109.970
1100	586.909	697.083	121.191
1200	596.504	706.847	132.412
1300	605.341	715.829	143.634
1400	613.534	724.146	154.857
1500	621.170	731.889	166.079
1600	628.318	739.132	177.302

Table B₅. Thermodynamic functions of Cs₃I₂⁺, isomer II (cyclic)

<i>T</i>	Φ°	<i>S</i> [°]	<i>H</i> [°] (<i>T</i>) – <i>H</i> [°] (0)
298.15	428.610	528.018	29.638
700	515.792	620.054	72.983
800	529.746	634.476	83.784
900	542.103	647.199	94.586
1000	553.192	658.582	105.390
1100	563.248	668.879	116.194
1200	572.448	678.281	127.000
1300	580.926	686.930	137.805
1400	588.788	694.939	148.612
1500	596.115	702.394	159.418
1600	602.978	709.369	170.225

Table B₆. Thermodynamic functions of Cs₂I₃⁻, isomer II (cyclic)

<i>T</i>	Φ°	<i>S</i> [°]	<i>H</i> [°] (<i>T</i>) – <i>H</i> [°] (0)
298.15	438.302	537.833	29.675
700	525.557	629.876	73.023
800	539.519	644.299	83.824
900	551.882	657.022	94.626
1000	562.975	668.405	105.430
1100	573.035	678.703	116.235
1200	582.238	688.105	127.040
1300	590.719	696.754	137.846
1400	598.582	704.762	148.652
1500	605.912	712.218	159.459
1600	612.777	719.193	170.266

Table B₇. Thermodynamic functions of Cs₃I₂⁺, isomer III (bipyramidal)

<i>T</i>	Φ°	<i>S</i> [°]	<i>H</i> [°] (<i>T</i>) – <i>H</i> [°] (0)
298.15	391.065	489.077	29.222
700	486.032	589.692	72.562
800	499.910	604.113	83.362
900	512.209	616.836	94.164
1000	523.251	628.219	104.968
1100	533.269	638.516	115.772
1200	542.437	647.918	126.577
1300	550.889	656.567	137.382
1400	558.726	664.575	148.189
1500	566.034	672.031	158.995
1600	572.879	679.005	169.802

Table B₈. Thermodynamic functions of Cs₂I₃⁻, isomer III (bipyramidal)

<i>T</i>	Φ°	<i>S</i> [°]	<i>H</i> [°] (<i>T</i>) – <i>H</i> [°] (0)
298.15	401.919	500.054	29.259
700	488.365	592.077	72.599
800	502.251	606.499	83.399
900	514.554	619.221	94.200
1000	525.600	630.604	105.004
1100	535.621	640.901	115.808
1200	544.792	650.303	126.613
1300	553.245	658.952	137.419
1400	561.085	666.960	148.225
1500	568.395	674.416	159.031
1600	575.241	681.390	169.838

© 2015 Mwanga et al.; This is an Open Access article distributed under the terms of the Creative Commons Attribution License (<http://creativecommons.org/licenses/by/4.0>), which permits unrestricted use, distribution, and reproduction in any medium, provided the original work is properly cited.

Peer-review history:

The peer review history for this paper can be accessed here:
<http://www.sciencedomain.org/review-history.php?iid=1137&id=5&aid=9221>